



1           **Technical note: Accelerate coccolith size separation via**  
2   **repeated centrifugation**

3

4                           Hongrui Zhang<sup>1,2</sup>, Chuanlian Liu<sup>1</sup>, Luz Maria Mejia<sup>2</sup>, Heather Stoll<sup>2</sup>

5           1. State Key Laboratory of Marine Geology, Tongji University, Shanghai, 200092, China

6           2. Geological Institute, Department of Earth Science, Sonneggstrasse 5, ETH, 8092, Zürich, Switzerland

7           Corresponding to: Hongrui Zhang ([103443\\_rui@tongji.edu.cn](mailto:103443_rui@tongji.edu.cn); [zh@ethz.ch](mailto:zh@ethz.ch))

8           **Abstract:**

9           Coccolithophore play a key role in the marine carbon cycle and ecosystem. The  
10           carbonate shells produced by coccolithophore, named as coccolith, could be well  
11           preserved in the marine sediment for million years and become an excellent archive for  
12           paleoclimate studies. The micro filtering and sinking-decanting method have been  
13           successfully designed for coccolith separation and promoted the development of  
14           geochemistry studies on coccolith, such as the stable isotopes and Sr/Ca ratio. However,  
15           these two methods are still not efficient enough for the sample-consuming methods. In  
16           this study, the trajectory of coccoliths movement during a centrifugation process was  
17           calculated in theory and carefully tested by separations in practice. We offer a matlab  
18           code to estimate the appropriate parameter, angular velocity at a fixed centrifugation  
19           duration, for separating certain coccolith size fractions from bulk sediment. This work  
20           could improve the efficiency of coccolith separation, especially for the finest size  
21           fraction and make it possible to carry the clumped isotope and radio carbon analysis on  
22           coccolith in sediment.

23



## 24 1. Introduction

25 Cocolithophores are a group of marine calcifying eukaryotic phytoplankton.,  
26 whose calcite exoskeletons (i.e. coccolith) contribute significantly to the particulate  
27 inorganic carbon (PIC) export from the euphotic zone into the deep ocean (Young and  
28 Ziveri, 2000). Coccoliths preserved in marine sediment are also excellent archive for  
29 paleo-productivity reconstruction (Beaufort et al., 1997). The element ratio, Sr/Ca, in  
30 coccolith is correlated with the growth rate of calcite crystal (Stoll et al., 2002) thereby  
31 becoming a competitive candidate for coccolithophore growth rate which is an essential  
32 parameter in the paleo-CO<sub>2</sub> reconstruction by alkenone carbon isotope. However, the  
33 coccolith geochemical analyses are limited by the difficulty of separating coccolith  
34 from bulk sediment. To solve this problem, different separating methods have been  
35 proposed in the past a few decades (Paull and Thierstein, 1987; Stoll and Ziveri, 2002;  
36 Minoletti et al., 2008).

37 Most of them, in general, could be categorized into two groups: the first one is  
38 micro-filtering and the second is sinking-decanting technique. The micro-filtering  
39 method relies heavily on the specifications of micro filter membrane (such as 3µm, 5µm  
40 and 8µm pore size), which is highly effective in separation of the larger size coccoliths,  
41 but useless for coccolith smaller than 2µm. The sinking-decanting method, on the other  
42 hand, could offer more freedom in coccolith size by adjusting the sinking durations,  
43 thereby separating both small and large coccoliths. However, because of the slow  
44 sinking speed, a single separation of particles smaller than 2 µm may take more than 10  
45 hours in settling. Moreover, about 6–8 times operations should be repeated, which  
46 means a full separation may takes at most one week. Hence, it is necessary to improve  
47 this method by reducing the time cost in coccolith separation.

48 Based on the Stokes sinking equation, the sinking rate of a certain particle  
49 increases with the increase of density difference between particle and liquid, decrease  
50 of the liquid viscosity and the increase of gravity. Changing the physical property of  
51 liquid often leads to the organic and toxic solvent which could lead to potential



52 contaminations for the further geochemistry analyses. A better way to accelerate  
53 coccolith sinking speed is changing the gravity, or the acceleration speed of the  
54 reference system, which can be easily achieved by centrifugation. One study has  
55 mentioned the usage of centrifugation in coccolith separation, but only centrifugation  
56 settings for a special case were provided (Hermoso et al., 2015). Here in this study, the  
57 method of separation coccolith by centrifugation is introduced systemically. We first  
58 calculate the trajectory of coccolith movement in a centrifugation processes and show  
59 how to estimate the centrifugation parameters in different situations. After that, two  
60 tests are performed to confirm the robustness of our calculations. Ultimately, a sample  
61 containing coccoliths ranging from 2  $\mu\text{m}$  to 12  $\mu\text{m}$  is selected for a separation case in  
62 practice.

## 63 2. Trajectory of coccoliths during centrifugation

64 The movement of coccolith in centrifugation is similar to that under the gravity.  
65 Previously, we have calculated the separation ratio variation with time during the  
66 settling (Zhang et al., 2018). All calculations in this study are with an assumption that  
67 the coccolith is in the force balance all the time during both settlings and centrifugations  
68 for a convenience of calculation. Here we offer a brief proof for this assumption and do  
69 a quick review of derivation we did before.

70 Based on the Newton second law, the force balance of a sphere object during  
71 sinking can be described by the following equation:

$$72 \quad F = \frac{4}{3}\pi r^3 \rho_p g - \frac{4}{3}\pi r^3 \rho_l g - 6\pi\eta r v = \frac{4}{3}\pi r^3 \rho_p \frac{dv}{dt} \quad (\text{Eq. 1.})$$

73 where  $F$  is the join force of particle, which is equal to zero in force balance,  $r$  is  
74 the radius of sphere,  $\rho_p$  and  $\rho_l$  are the density of particle and liquid, respectively,  $\eta$  is  
75 the viscosity of liquid and  $v$  is the particle sinking speed,  $dv/dt$  is the particle acceleration  
76 speed, which can be also marked as  $a$ . On the right side of the first equal mark, the first  
77 term is the gravity force, the second term is buoyancy and the third term is the dragging



78 force from liquid. Transform Eq. 1, we can obtain the expression of accelerated speed  
79 ( $a = F/m$ ) of sphere as Eq. 2:

$$80 \quad a = \frac{dv}{dt} = -\frac{9\eta}{2r^2}v + \frac{g}{\rho_{cal}}(\rho_p - \rho_l) \quad (\text{Eq. 2.})$$

81 Given the initial value of sinking speed is equal with zero at the initial time ( $t = 0$ ),  
82 we can solve the differential equation Eq. 2 and obtain the variation of velocity with  
83 time as following equation:

$$84 \quad v = \frac{-e^{\left[-\frac{9\eta}{2r^2}t + \ln\left(-\frac{g}{\rho_{cal}}(\rho_p - \rho_l)\right)\right]} + \frac{g}{\rho_{cal}}(\rho_p - \rho_l)}{\frac{9\eta}{2r^2}} \quad (\text{Eq. 3.})$$

85 when the value of  $t$  is large enough, the first term of numerator in Eq. 3 is close to  
86 zero, which represents the sinking velocity is close to the termination sinking velocity  
87 described in Stocks equation (Eq. 4).

$$88 \quad \lim_{t \rightarrow \infty} v = \frac{2(\rho_p - \rho_l)gr^2}{9\eta} \quad (\text{Eq. 4.})$$

89 Given the particle as a 5  $\mu\text{m}$  in radius calcite carbonate sphere with a density of  
90 2.7  $\text{g cm}^{-3}$  and the density of water is equal to 1.0  $\text{g cm}^{-3}$ , when the  $t$  is equal to  $10^{-7}$  s,  
91 the first term of numerator is  $3.7 \times 10^{-44} \text{ m s}^{-2}$  and small enough to be neglected compared  
92 with the second term, which is 6.3  $\text{m s}^{-2}$ . The time scale in coccolith separation is minute  
93 for centrifugation and hour for settling, therefore we suggest that it is reasonable to  
94 assume the coccolith sinks with the ‘terminal speed’ from the very beginning.

95 The only difference between the terminal speed in centrifugation and under gravity  
96 is the acceleration speed. If the  $g$  in Eq. 1 - 4 is adapted by  $a$ , which is the acceleration  
97 speed of coccolith during centrifugation, these four equations above can also describe  
98 the sphere movement in the centrifugation if we adapt the gravity to centripetal  
99 acceleration ( $ca$ ). Here we define a new parameter named as Sinking Parameter ( $sp$ ):

$$100 \quad sp = \frac{v}{g} \quad (\text{Eq. 5.})$$



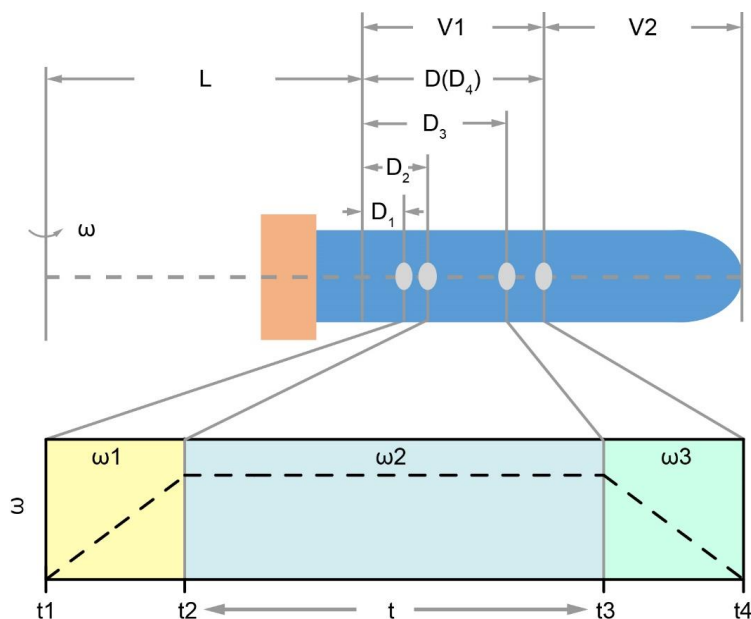
101 The physical meaning of  $sp$  is the influence of coccolith shape and liquid property  
102 (density and viscosity) on sinking velocity without considering the effect of gravity (or  
103 the acceleration rate of reference system). The sinking speed of coccolith in water  
104 during a centrifugation ( $v'$ ) can be described as following:

$$105 \quad v' = sp \times ca = sp \times \omega^2 \times (L + D) \quad (\text{Eq. 6.})$$

106 where the  $ca$  is centripetal acceleration during centrifugation,  $\omega$  is angular velocity  
107 of centrifuge, the  $(L+D)$  is the rotation radius as illustrated in **Figure 1**. The  $L$  is a  
108 fixed value for a certain type of centrifuge and the  $D$  depended on the position of  
109 coccolith in the tube. Here we should notice two issues: the first one is that the rotation  
110 radius is varying when coccolith is moving in the centrifuge tube, in other words,  $D$  is  
111 always changing. This effect could be ignored when the  $L$  is much larger than  $D$ , but,  
112 unfortunately, most of centrifuge employed in geochemistry laboratory is not large  
113 enough. The second one is the angular velocity is dynamic during when the centrifuge  
114 is accelerating and decreasing. To solve these two dynamic parameters, Eq.6 was  
115 transformed into a form of differential equation as Eq. 7 for the convenience of  
116 integration in the next step.

$$117 \quad dt = \frac{dD}{v} = \frac{dD}{sp \times \omega^2 \times (L + D)} \quad (\text{Eq. 7.})$$

118 For all centrifugations there are three stages: the acceleration stage ( $t_1$  to  $t_2$  in  
119 Figure 1), the constant angular velocity stage ( $t_2$  to  $t_3$  in Figure 1) and the deceleration  
120 stage ( $t_3$  to  $t_4$  in Figure 1). The duration of acceleration stage and deceleration stage can  
121 usually be controlled and the angular velocity is changing with a constant speed. For  
122 those machines which the angular velocity dynamic ( $\omega=f(t)$ ) is unknown we should  
123 measure it manually.



124

125 **Figure 1.** The position of coccolith and the variation of  $\omega$  in the three centrifuging stages:  $L$   
 126 represents the minimum rotation radius, the  $V_1$  and  $V_2$  represent the volume of two parts; in the  
 127 first stage, the angular velocity increases from zero to  $\omega_1$  (it could be linear or cubic, which  
 128 depends on the machine). Meanwhile the coccolith moves a distance of  $D_2 - D_1$ ; similarly, the  
 129 coccolith moves a distance of  $D_3 - D_2$  in the second stage and it march a distance of  $D_4 - D_3$  in the  
 130 last stage.

131 After knowing the angular velocity curve, integrate the  $D$  over  $t$  in the Eq. 7 by  
 132 three steps from  $t_1$  to  $t_4$ :

133 
$$sp \times \int_{t_1}^{t_2} \omega_1^2 dt = \ln^{(L+D_2)} - \ln^{(L+D_1)} \quad (\text{Eq. 8.})$$

134 
$$sp \times \int_{t_2}^{t_3} \omega_2^2 dt = \ln^{(L+D_3)} - \ln^{(L+D_2)} \quad (\text{Eq. 9.})$$

135 
$$sp \times \int_{t_3}^{t_4} \omega_3^2 dt = \ln^{(L+D_4)} - \ln^{(L+D_3)} \quad (\text{Eq. 10.})$$

|



136 Add the Eq. 8 – 10 together gives:

$$137 \quad sp \times \left( \int_{t_1}^{t_2} \omega_1^2 dt + \int_{t_2}^{t_3} \omega_2^2 dt + \int_{t_3}^{t_4} \omega_3^2 dt \right) = \ln^{(L+D_4)} - \ln^{(L+D_1)} \quad (\text{Eq. 11.})$$

138 Set  $D_4$  equal to  $D$ , which represents the maximum distance that a coccolith can  
 139 move in the upper suspension  $V_1$ . Now we can use the coccolith sinking property,  $sp$ ,  
 140 and centrifugation settings to describe the coccolith position after centrifugation  $D_1$ :

$$141 \quad D_1 = \frac{L + D}{e^{[sp \times (\int_{t_1}^{t_2} \omega_1^2 dt + \int_{t_2}^{t_3} \omega_2^2 dt + \int_{t_3}^{t_4} \omega_3^2 dt)]}} - L \quad (\text{Eq. 12.})$$

142 The meaning of  $D_1$  is all coccolith with an initial position on the right side of  $D_1$   
 143 in **Figure 1** will move to the right side of  $D_4$  and then be kept in the suspension after  
 144 pumping, while the coccolith on the left side of  $D_1$  will be removed by pumping.

145 In our previous publication (Zhang et al., 2018), we defined a parameter named as  
 146 separation ratio ( $R$ ), which represents the percentage of coccolith removed in one  
 147 separation if we pump the upper  $V_1$  volume suspension out of  $(V_1 + V_2)$  suspension in  
 148 total.

$$149 \quad R = \frac{V_1 \times \frac{D_1}{D}}{V_1 + V_2} \quad (\text{Eq. 13})$$

150 Replacing the  $D_1$  in Eq. 15 with Eq. 12 gives the separation ratio ( $R$ ) as a function  
 151 of centrifugation settings:

$$152 \quad R = \frac{V_1}{V_1 + V_2} \times \frac{1}{D} \times \left( \frac{L + D}{e^{[sp \times (\int_{t_1}^{t_2} \omega_1^2 dt + \int_{t_2}^{t_3} \omega_2^2 dt + \int_{t_3}^{t_4} \omega_3^2 dt)]}} - L \right) \quad (\text{Eq. 14})$$

153 The  $R$  can be employed in estimating the centrifugation parameters for separating  
 154 one type of coccoliths from another. For example, if we want to separate a group of  
 155 coccolith (marked as Coccolith<sub>A</sub>, with sinking parameter  $sp_A$ ) from another group of  
 156 coccolith (marked as Coccolith<sub>B</sub>, with sinking parameter of  $sp_B$  and  $sp_A < sp_B$ ), the  $R$  of  
 157 Coccolith<sub>B</sub> should be set as zero, which means all Coccolith<sub>B</sub> in the section  $V_1$  have  
 158 sunk into  $V_2$  after centrifugation and therefore all coccolith pumped out should be



159 Coccolith<sub>A</sub>. To solve the angular velocity ( $\omega_2$ ) and centrifugation duration ( $t = t_3 - t_2$ ) in  
160 Eq.14, we need to fix at least one of them. Usually the duration could be safely set as 1  
161 min or 2 min, then solve the suitable angular velocity with known parameters  $V_1$ ,  $V_2$ ,  
162  $D$  and  $L$ . The matlab code for the parameter estimation is in attachment. After repeating  
163 these ‘centrifugation-pumping’ routines several times, the Coccolith<sub>A</sub> could be fully  
164 separated from Coccolith<sub>B</sub>.

### 165 **3. Test of the correctness of calculations**

#### 166 **3.1 Experimental design**

167 To test the robustness of our estimation in the last section, we performed two  
168 groups of experiments comparing the observed with predicted separation ratio. Here we  
169 select two different coccoliths, *F. profunda* and small *Gephyrocapsa*, with small size  
170 and thereby slow sinking speed sampled from ODP 807 and IODP U1304, respectively.  
171 Most of small *Gephyrocapsa* employed in this study are smaller than  $3 \mu\text{m}$  with a  
172 mixture of *G. muelleriae* less than 10%. Two centrifuges from Anting Company, TDL–  
173 40B and DL–5B, were selected to perform the tests. The angular velocity of DL–5B can  
174 be set as linear increased or decreased with time in the acceleration or deceleration  
175 stages, while the angular velocity of TDL–40B was measured manually by reading the  
176 number on the instrument panel. The centrifugation duration can only be adapted by a  
177 step of one minute on both of these two machines. The slowest angular velocities of  
178 these two machines are 500 revolutions per minute (rpm). If we selected the water as  
179 dispersion agent, most of the coccolith we used will sink to the tube bottom after two  
180 minutes even with the slowest angular velocity. Hence, to slow down the coccolith  
181 sinking speed in these tests, glycerol solution was employed in this equation test, which  
182 can be dissolved with water in any proportion and washed away from carbonate calcite  
183 particles conveniently. The density and viscosity data can be found in **Table 1**.

184 All calculations above are for the situation that particles sinking in the water or the  
185 diluted solution, the physical property of which is close to water. However, in this case,





186 the property of glycerol is significant different with water. Here we define a new  
187 parameter,  $\tau$ , to transform the sinking speed in water to that in different liquid. The  
188 physical meaning of  $\tau$  is a ratio turning the sinking velocity in water ( $v$ ) to the velocity  
189 in any liquid with different density and viscosity ( $v'$ ):

$$190 \quad v' = v \times \tau \quad (\text{Eq. 15})$$

191 Based on the definition of Stokes equation, the term  $\tau$  can be calculated as  
192 following:

$$193 \quad \tau = \frac{(\rho_p - \rho_l)}{(\rho_p - \rho_w)} \times \frac{\eta_w}{\eta_l} \quad (\text{Eq. 16})$$

194 where the  $\rho_p$ ,  $\rho_l$  and  $\rho_w$  are density of particle, liquid (in this study is glycerol  
195 solution) and water; the  $\eta_l$  and  $\eta_w$  are the viscosity of liquid and water.

196 Combine the Eq. 14–16 forming the separation ratio as a function of centrifugation  
197 settings in different liquid:

$$198 \quad R = \frac{V_1}{V_1 + V_2} \times \frac{1}{D} \times \left( \frac{L + D}{e^{\left[ \frac{v}{g} \times \frac{(\rho_p - \rho_l)}{(\rho_p - \rho_w)} \times \frac{\eta_w}{\eta_l} \times \left( \int_{t_1}^{t_2} \omega_1^2 dt + \int_{t_2}^{t_3} \omega_2^2 dt + \int_{t_3}^{t_4} \omega_3^2 dt \right) \right]}} - L \right) \quad (\text{Eq. 17})$$

199 In this test, the calculated R by Eq. 17 will be compared with measured one. To  
200 perform these tests, about 100 mg bulk sediments were scattered into 30 ml 0.5%  
201 ammonia and, after that, particles larger than 20  $\mu\text{m}$  particles were removed by mesh.  
202 In this test, we should obtain suspensions with nearly monospecific coccolith. To  
203 achieve it, in the test with *F. profunda*, coccoliths larger than 3  $\mu\text{m}$  were removed by  
204 the sinking method described in Zhang et al. (2018) and coccoliths larger than 5  $\mu\text{m}$   
205 were removed by the same method in the test with small *Gephyrocapsa*. Briefly, the  
206 suspension was (1) set in a 100 ml Reagent bottle sinking freely for a few hours, and  
207 then (2) pumped out the upper 2cm. Repeat these two steps for 5–8 times until  
208 coccoliths were purified. The sinking duration was 2 hours for *F. profunda* sample and  
209 1.25 hours for small *Gephyrocapsa* sample, respectively.



210 Then 50 ml tubes with 45 ml coccolith suspensions were mounted in the centrifuge  
 211 and run with the settings shown in Table 1. After centrifugation, the upper 30 ml  
 212 supernatant was pumped out by pipette and then filtered onto 0.4  $\mu\text{m}$  polycarbonate  
 213 member with a vacuum pump. The coccoliths on polycarbonate membrane were  
 214 resuspended into 20 ml diluted ammonia again and coccoliths number in the suspension  
 215 was measured with the same method described in our previous work (Zhang et al.,  
 216 2018). Finally, the separation ratio, R, was calculated by the coccolith number in the  
 217 upper 30 ml suspension divided by the total coccolith number. All the centrifuging  
 218 experiments were carried out in laboratory with temperature controlled around 20 ( $\pm 1$ )  $^{\circ}\text{C}$   
 219 to avoid the variation of physical properties, especially the viscosity, with temperature.

220 **Table 1.** The settings of two tests: the density and viscosity of glycerol in 20 $^{\circ}\text{C}$ , data from  
 221 Dorsey (1940); the parameters of centrifuge employed in this study: Fp and G60 represent the  
 222 experiment carried out with *F. profunda* in 70% glycerol and small *Gephyrocapsa* ( $< 3 \mu\text{m}$ ) in  
 223 60% glycerol, respectively; L represents the minima rotation radius of centrifugation, which  
 224 represents the distance between the shaft and top of suspension as illustrated in Figure 1; A, B and  
 225 C are the terms on the left side of equal mark in Eq. 8–10.

	glycerol (%)	$\eta$ (mPa s)	$\rho$ (g cm $^{-3}$ )	$\tau$	Centrifuge	L (cm)	A (s $^{-1}$ )	B (s $^{-1}$ )	C (s $^{-1}$ )
<b>Fp</b>	70%	22.5	1.16	0.040	TDL40B	6.2	$1.060 \times 10^6$	$9.867 \times 10^4 \times t$	$1.937 \times 10^6$
<b>G60</b>	60%	10.8	1.14	0.084	DL-5B	8.37	$7.457 \times 10^5$	$9.867 \times 10^4 \times t$	$2.193 \times 10^6$

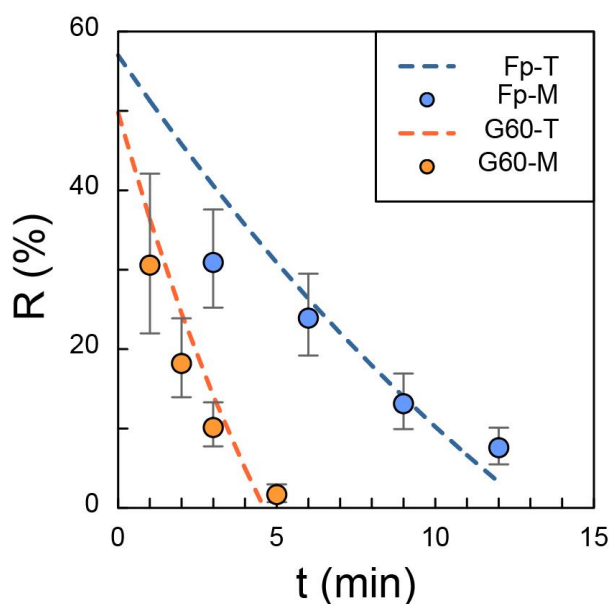
### 226 3.2 Result of experiments

227 In the test, 30 ml suspension was pumped out from 45 ml suspension leading to  
 228 the initial R should be 60%. However, the intercept of calculated R is smaller than 60%  
 229 as the gravity settling in Zhang et al. (2018), because the time in the x-axis of Figure 2  
 230 is the period in which angular velocity remains constant. In other words, even the time  
 231 is set as zero, the centrifuge will still do the acceleration and deceleration processes and  
 232 coccolith will move toward the bottom. The results of observed R (dots in **Figure 2**)  
 233 are close to the theoretical values (dash lines in **Figure 2**), though a few measured



234 results are lower than prediction. We suggested that this difference may be caused by  
235 coccolith loss during harvesting of the coccolith from glycerol solutions into ammonia  
236 solution.

237 So far, we have obtained the coccolith movement equation in the centrifugation  
238 and prove its correctness. In the next section, a case of coccolith separation by  
239 centrifuging method will be carried out giving an example of separation.



240

241 **Figure 2.** The comparison of theoretical and measured separation ratio (R): the dots  
242 represent the measured values and dish lines are theoretical calculations. The error bars represent  
243 95% error based on the assumption that the error of counting coccolith follows the Poisson  
244 distribution. The orange dots represent the measured R in small *Gephyrocapsa* with 60% glycerol  
245 test (G60-M) and the blue ones represent the measured R in *F. profunda* with 70% glycerol test  
246 (Fp-M). The orange dashed line is the theoretical values for small *Gephyrocapsa* with 60%  
247 glycerol test (G60-T) and the blue one is the theoretical values for *F. profunda* with 70% glycerol  
248 test (Fp-T). The raw pictures for coccolith counting were shown in **Figure S1** and **S2**.

#### 249 4. Separation of coccoliths in practice

|



#### 250 4.1 Separation steps

251 The aim of this section is using the centrifugation method to separate a sample in  
252 practice. A sample from ODP 982B (56X Section 5 5-9cm) dated around mid-Miocene  
253 (nannofossil zoon NN4) was selected in this test. The coccolithophore *Reticulofenestra*  
254 spp. dominated in the assemblage, with long axis length ranging from 2  $\mu\text{m}$  to more  
255 than 12  $\mu\text{m}$ , offering an ideal sample to test the coccolith separation method.  
256 *Calcidiscus* spp. (4–10  $\mu\text{m}$ ), *Helicosphaera* spp. (5–10  $\mu\text{m}$ ) and *Coccolithus* spp. (6–8  
257  $\mu\text{m}$ ) were also found in this sample, which contributed less than 10% of all coccoliths  
258 together. The preservation of fossil was moderate with many coccolith fragments but  
259 no evidence of dissolution in the raw sample. The detailed operations are as following:

260 **Step 1:** weigh about 40 mg bulk sediment, scatter with 45ml 0.5% ammonia  
261 solution and transfer the suspension into a 50 ml centrifuging tube;

262 **Step 2:** Calculate the centrifugation parameters (angular velocity and duration).  
263 Here we did not measure coccolith sinking velocities, but employ the length-velocity  
264 relationship in the previous study directly: sinking rate at 25°C =  $0.0982 \times \text{length}^2$  (Zhang  
265 et al., 2018). Based on this length-velocity equation and the centrifuge properties listed  
266 in **Table 1**, we estimated that the angular velocity and duration for separating coccolith  
267 with a length of 2  $\mu\text{m}$ , 3  $\mu\text{m}$ , 5  $\mu\text{m}$ , 8  $\mu\text{m}$  and 10  $\mu\text{m}$  should be 1850 rpm 2 min, 2250  
268 rpm 1 min, 1400 rpm 1min, 1000 rpm 1min and 600 rpm 1min, respectively. The  
269 Matlab code for calculating the angular velocity at fixed centrifugation duration (1 or 2  
270 minutes) are in the supplementary.

271 **Step 3:** Mount the tube into the centrifuge and balance weight, set the angular  
272 velocity as 1850 rpm and the duration as 2 minutes and start the machine;

273 **Step 4:** Pump out the upper 30 ml suspensions and remove them into a beaker (500  
274 ml or larger beaker, depends how many times repeating this step) and drop about 100  
275  $\mu\text{l}$  onto a glass cover. Dry the suspension on glass cover and mount the cover on slider.  
276 The details in this step follow Bordiga et al. (2015);

277 **Step 5:** Repeat Step 2–5 with different centrifugation parameters listed in Table 2;



278           **Step 6:** Take pictures of coccoliths in each slider on microscope and measure the  
279 coccolith size on computer with the method described by Fuertes et al. (2014).

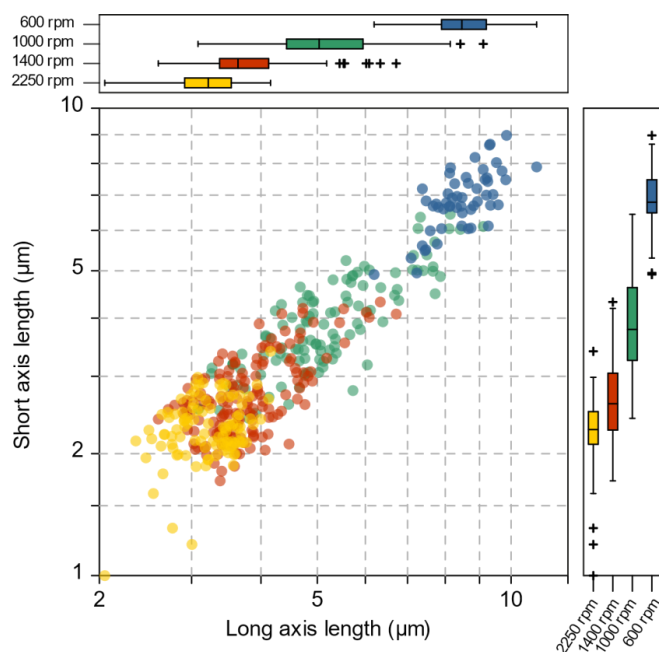
280

281           **Table 2.** Centrifugation parameters in the Miocene coccolith separations

	<2 $\mu\text{m}$	2–3 $\mu\text{m}$	3–5 $\mu\text{m}$	5–8 $\mu\text{m}$	8–10 $\mu\text{m}$
Angular velocity ( $\omega_2$ , rpm)	1850	2250	1400	1000	600
Duration ( $t = t_3 - t_2$ , s)	120	60	60	60	60

#### 282   **4.2 Coccolith length in each fraction**

283           The coccolith size distribution harvested from different centrifugation settings are  
284 shown in **Figure 3** (the coccolith size was measured in circular polarizing microscope  
285 and coccoliths under cross polarizing microscope were shown in **Figure S3-S9** for  
286 species identification). The results show that the separated coccolith size increased with  
287 the decrease of angular velocity and the differences of mean coccolith lengths are  
288 significant between each size fractions. However, we should also notice that there is  
289 still overlap of coccolith sizes between two neighbouring fractions. With the  
290 centrifugation parameters set as 2250 rpm and 2 min, the coccoliths harvested have  
291 long axis lengths around 2–4  $\mu\text{m}$  and when the centrifugation parameters was varied to  
292 1400 rpm and 1 min, the coccolith long axis size ranges from 3  $\mu\text{m}$  to 7  $\mu\text{m}$ , which  
293 means coccoliths with a length between 3–4  $\mu\text{m}$  appear in two fractions. Such situations  
294 may also happen in both settling and micro filtering methods, but the range of overlap  
295 seems to be larger for the centrifugation method compared with the size fractions  
296 harvested by other methods.



297

298 **Figure 3.** The coccolith size in different fraction after centrifuging separation: the yellow,  
299 red, green and blue dots represent 2250 rpm-2min, 1400 rpm-1min, 1000 rpm-1min and 600 rpm-  
300 1min, respectively.

301

### 302 4.3 Troubleshooting

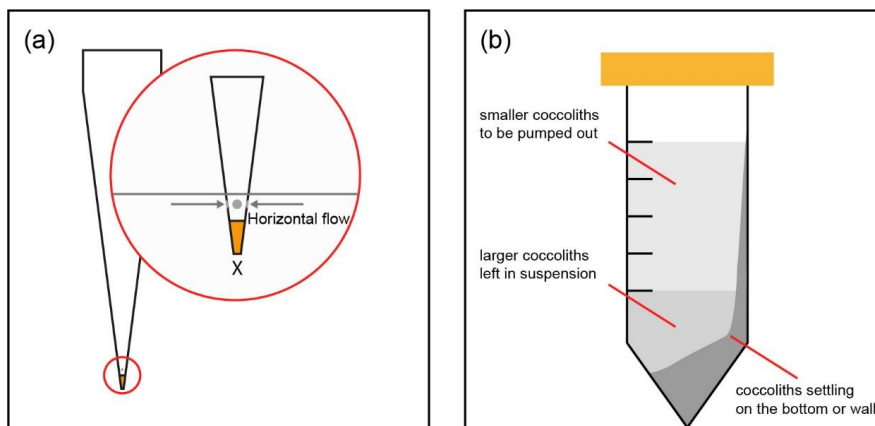
303 The first potential reason leading to overlap may be the repeating times are not  
304 enough. This could be the main problem for settling under gravity, since the time costs  
305 for separation under gravity is much larger than the centrifugation method. Bolton et al.  
306 (2012) suggested that 4–6 times separations are enough for fossil extraction and in our  
307 separations, we repeated more than 8 times for a certain centrifugation setting.  
308 Considering these facts, we suggest that this overlapping was not caused by the  
309 separation times.

310 Another reason could be that larger coccoliths, which are supposed to sink into the  
311 lower suspension, are pumped out after centrifugation. When the upper suspension was



312 pumped out, the pumping speed could be too fast drawing up larger coccolith from the  
313 lower suspension. This problem could be solved by reducing the pumping speed.  
314 However, in practice, the pumping speed of pipette is difficult to control. Here we  
315 recommend to modify the tips of pipette as following steps: (1) suck a drop of glue into  
316 the top of pipette tips (the Norland optical adhesive 74 was employed in this study); (2)  
317 solidify the glue with ultraviolet ray to seal the top of tips; (3) drill holes above the glue  
318 horizontally. After this modification, the suspension will go into tips horizontally  
319 instead of vertically (**Figure 4a**) to avoid mixing larger coccoliths with smaller ones.

320 The size overlapping could also be caused by the centrifugation tube not remaining  
321 perfectly horizontal during centrifugation. In our calculations, the tubes are assumed to  
322 be perfectly horizontal during all centrifugation processes and, thereby it was assumed  
323 that there should be no collisions between coccoliths and tube wall nor among  
324 coccoliths. However, in practice, the tubes in centrifuge are not always horizontal and  
325 even a few degrees slope of the tubes can lead some coccoliths to knock and stick on  
326 the tube wall forming a significant coccolith layer on one side of tube wall as illustrated  
327 in **Figure 4b**. These coccoliths on tube wall will be pumped out after centrifugation  
328 causing the coccolith length overlapping among two fractions. To avoid this problem,  
329 before the step of pumping out suspension, we should observe the tube carefully. If a  
330 coccolith layer can be found on the tube wall, the pipette tip should be placed on the  
331 opposite of the coccolith layer to reduce the size overlapping.





333 **Figure 4.** Two methods to reduce the coccolith size overlapping. (a) Adaption of pipette tip:  
334 the orange part on tip represents sealed by solidified glue and the gray parts mean that small holes  
335 should be drilled allowing the suspension flowing in horizontally; (b) Choose a property pumping  
336 position to avoid extracting the coccolith on tube wall: the lightest gray part in the tube represents  
337 the suspension in which the smaller coccolith floats, most of the larger coccoliths are in the lower  
338 part of the suspension and the tube bottom.

## 339 **5. Summary**

340 In this study, we described the method of separating coccolith from bulk sediment  
341 by centrifuge. The rotation speed for separating coccoliths within a certain range of  
342 length could be solved after measuring the rotations radium (property of centrifuge)  
343 and fixing the centrifugation duration.

344 The centrifugation method is not perfect accurate and could still mix different  
345 species of coccolith as other traditional separating methods. The size overlapping of  
346 this method could be reduced by adapting the pipette tips and avoiding pumping the  
347 coccolith on tube well out. However, this method is more efficient in separating the  
348 finest particle (smaller than 3  $\mu\text{m}$ ) out of bulk sediment, which is always the time-  
349 consuming step in micro-filtering and sinking method. Thereby, this method can be  
350 widely used in the sample preparation for analyses needing a large amount of material,  
351 such as coccolith clumped isotope and radioactive carbon isotope measurement.  
352 Moreover, the centrifugation method can be combined with other separation steps, for  
353 example using the centrifugation method to remove the finest particles followed by  
354 micro filtering with different size of membrane. This method could largely reduce the  
355 time cost in sample preparation for coccolith geochemistry analyses and have the  
356 potential for wide use in the future.

## 357 **References**





- 358 Beaufort, L., Lancelot, Y., Camberlin, P., Cayre, O., Vincent, E., Bassinot, F. and  
359 Labeyrie, L.: Insolation cycles as a major control of equatorial Indian Ocean  
360 primary production, *Science* 278, 1451-1454.  
361 <https://doi.org/10.1126/science.278.5342.1451>, 1997.
- 362 Bolton, C.T., Stoll, H.M. and Mendez-Vicente, A.: Vital effects in coccolith calcite:  
363 Cenozoic climate-pCO<sub>2</sub>drove the diversity of carbon acquisition strategies in  
364 coccolithophores? *Paleoceanography* 27. <https://doi.org/10.1029/2012pa002339>,  
365 2012.
- 366 Bordiga, M., Bartol, M. and Henderiks, J.: Absolute nannofossil abundance estimates:  
367 Quantifying the pros and cons of different techniques. *Revue de*  
368 *micropaléontologie* 58, 155-165, <https://doi.org/10.1016/j.revmic.2015.05.002>,  
369 2015.
- 370 Dorsey, N.E. (1940) *Properties of ordinary water-substance*. Reinhold Publishing  
371 Corporation.; New York.
- 372
- 373 Fuertes, M.-Á., Flores, J.-A. and Sierro, F.J.: The use of circularly polarized light for  
374 biometry, identification and estimation of mass of coccoliths. *Marine*  
375 *Micropaleontology* 113, 44-55, <https://doi.org/10.1016/j.marmicro.2014.08.007>,  
376 2014.
- 377 Hermoso, M., Candelier, Y., Browning, T.J. and Minoletti, F.: Environmental control  
378 of the isotopic composition of subfossil coccolith calcite: Are laboratory culture  
379 data transferable to the natural environment? *GeoResJ* 7, 35-42,  
380 <https://doi.org/10.1016/j.grj.2015.05.002>, 2015.
- 381 Minoletti, F., Hermoso, M. and Gressier, V. Separation of sedimentary micron-sized  
382 particles for palaeoceanography and calcareous nannoplankton biogeochemistry.  
383 *Nature protocols* 4, 14-24. <https://doi.org/10.1038/nprot.2008.200>, 2009
- 384 Paull, C.K. and Thierstein, H.R.: Stable isotopic fractionation among particles in  
385 Quaternary coccolith-sized deep-sea sediments. *Paleoceanography* 2, 423-429,  
386 <https://doi.org/10.1029/PA002i004p00423>, 1987.



387 Stoll, H.M., Rosenthal, Y. and Falkowski, P.: Climate proxies from Sr/Ca of coccolith  
388 calcite: calibrations from continuous culture of *Emiliana huxleyi*. *Geochimica et*  
389 *Cosmochimica Acta* 66, 927-936, [https://doi.org/10.1016/S0016-7037\(01\)00836-](https://doi.org/10.1016/S0016-7037(01)00836-5)  
390 5, 2002.

391 Stoll, H.M. and Ziveri, P.: Separation of monospecific and restricted coccolith  
392 assemblages from sediments using differential settling velocity. *Marine*  
393 *Micropaleontology* 46, 209-221, [https://doi.org/10.1016/S0377-8398\(02\)00040-3](https://doi.org/10.1016/S0377-8398(02)00040-3),  
394 2002.

395 Young, J.R. and Ziveri, P.: Calculation of coccolith volume and its use in calibration of  
396 carbonate flux estimates. *Deep sea research Part II: Topical studies in*  
397 *oceanography* 47, 1679-1700, [https://doi.org/10.1016/S0967-0645\(00\)00003-5](https://doi.org/10.1016/S0967-0645(00)00003-5),  
398 2000.

399 Zhang, H., Stoll, H., Bolton, C., Jin, X. and Liu, C. (2018) Technical note: A refinement  
400 of coccolith separation methods: measuring the sinking characteristics of  
401 coccoliths. *Biogeosciences* 15, 4759-4775, [https://doi.org/10.5194/bg-15-4759-](https://doi.org/10.5194/bg-15-4759-2018)  
402 2018, 2018.

#### 403 **Author contributions.**

404 This study was conceived by H.Z. and C.L. Measurements and calculations were  
405 conducted by H.Z. H.Z., H.S. and L.M. wrote the paper.

#### 406 **Acknowledgement**

407 This study was funded by National Science Foundation of China (41930536, to  
408 C.L.) ETH core funding (to H.S), European Union's Horizon 2020 research and  
409 innovation program under the Marie Skłodowska-Curie grant agreement (795053 to  
410 L.M.M.) and Chinese Scholarship Council (CSC) scholarship to H.Z. We thank the  
411 Integrated Ocean Drilling Program (IODP) for providing the samples. We thank Dr.  
412 Guodong Jia for providing two centrifuges to test our work and Xinquan Zhou for  
413 identification the Miocene nannofossils.